Mol Genet Genomics (2002) 268: 446–454
DOI 10.1007/s00438-002-0770-6

ORIGINAL PAPER

M. Saito · T. Awasaki · C. Hama

Genetic analyses of essential genes in cytological region 61D1–2 to 61F1–2 of *Drosophila melanogaster*

Received: 6 June 2002 / Accepted: 30 September 2002 / Published online: 5 November 2002

Abstract We performed a systematic mutagenesis screen for lethals in the genomic region 61D1–2 to 61F1–2 on chromosomal arm *3L* of *Drosophila melanogaster*. Our genetic analyses revealed that this region contains eight essential complementation groups including *trio*, *Glut1* and *extra macrochaetae* (*emc*). For the *trio* locus, 22 mutant alleles were identified, and all of the alleles analyzed resulted in defects in the central nervous system of embryos, indicating that *trio* functions in the control of axon extension or guidance. Western analysis showed that at least three proteins are derived from *trio* and also suggested that a polypeptide of over 200 kDa plays a crucial role in embryonic or larval development. In addition, a newly identified *emc* allele was associated with several defects in embryonic morphogenesis, including abnormalities in head involution, gut formation and dorsal closure, thus revealing multiple roles for *emc* in embryonic development. We also performed preliminary phenotypic analyses on stocks bearing mutations belonging to the other lethal complementation groups. These genes function in essential biological events, but the mutations do not result in gross morphological changes during embryonic stages. The present study extends our knowledge of the *Drosophila* gene set, by identifying most of the essential genes in the chromosomal region 61D1–2 to 61F1–2.

Keywords *Drosophila* · Mutagenesis · *trio* · *emc* · *Glut1*

Communicated by G. Reuter

M. Saito · T. Awasaki · C. Hama (✉)
Laboratory for Neural Network Development,
RIKEN Center for Developmental Biology,
2-2-3 Minatojima-minami, Chuo, Kobe,
Hyogo 650-0047, Japan
E-mail: hama@cdb.riken.go.jp
Fax: +81-78-3063235

M. Saito · T. Awasaki · C. Hama
Core Research for Evolutional Science and Technology,
Japan Science and Technology Corporation,
Kawaguchi, Saitama 332-0012, Japan

Present address: T. Awasaki
National Institute for Basic Biology,
Okazaki, Aichi 444-8585, Japan

Introduction

Among a variety of classical and modern methods for the isolation of mutations, chemical mutagenesis with ethyl methanesulfonate (EMS) and P-element insertion mutagenesis have most frequently been employed to identify genes in *Drosophila melanogaster*. Compared to the use of EMS, mutagenesis with P elements has the advantage of providing molecular tags for the genomic sequences, thus facilitating the physical mapping and cloning of the genes of interest. However, P-element insertion occurs unevenly along the chromosomes; a number of genomic regions do not seem to favor P-element integration, while limited regions known as hot spots are frequent insertion targets (Engels 1996). It is also known that transposon insertions tend to occur preferentially in regulatory regions and introns (Spradling et al. 1995). Thus, even when P-element mutagenesis is performed to apparent saturation, a considerable number of genes may remain genetically unidentified. Therefore, other methods must be used to complement P insertion techniques, in order to identify all the genes on the chromosomes. Mutagenesis with EMS has the advantage that this agent does not exhibit any apparent bias with respect to the loci or sequences mutagenized. In addition, single-base substitutions, which are frequently generated with EMS, sometimes result in temperature-sensitive or gain-of function phenotypes, which provide us with opportunities to obtain further insights into gene functions. Thus, EMS mutagenesis remains an important technique for identifying genes and revealing their functions, and eventually for understanding organisms in terms of the total complement of genetic information that they possess.

To understand the mechanism that regulates axon extension, we have made an effort to identify genes that

encode guanine nucleotide exchange factors (GEFs) for Rho family GTPases. Several lines of evidence have suggested that axon guidance is regulated by Rho family GTPases, including the classes typically represented by Rac, Cdc42 and Rho (reviewed in Luo 2000; Dickson 2001). Each of these molecules is suggested to play a characteristic role in regulating structural changes in the growth cone, a key structure for axon guidance. These GTPases are activated at the appropriate time and place by conversion from a GDP-bound to GTP-bound form, which is mediated by guanine nucleotide exchange factors (GEFs). Therefore, analyses of GEFs are necessary in order to understand the roles of signaling via Rho family GTPases in axon guidance. We took advantage of the *Drosophila* database to identify genes for GEFs, and found that the gene *trio* encodes a GEF that is expressed in the nervous system during axonal extension (Awasaki et al. 2000; see also Bateman et al. 2000; Liebl et al. 2000. Newsome et al. 2000). To elucidate the in vivo function of *trio*, we performed a systematic mutagenesis screen to identify mutations that fail to complement a deficiency that maps to cytological region 61D1–2 to 61F1–2 and uncovers the *trio* locus. We isolated 48 mutations that belong to eight complementation groups, including *trio*, *emc* and *Glut1* (which encodes a putative glucose transporter). The mutant phenotypes shown by many *trio* alleles confirm that *trio* plays an important role in axon extension. Moreover, an *emc* allele identified in this study was associated with multiple morphological defects in embryos, including aberrant head involution, gut formation and dorsal closure. We also carried out a preliminary analysis of the phenotypes associated with mutations in the other lethal complementation groups. The results indicated that these genes are involved in essential biological processes, but their mutants do not display any gross morphological changes – at least during embryonic stages. The analysis of these novel mutations will contribute to the goal of elucidating the functions of all essential *Drosophila* genes, which can now draw upon the wealth of sequence information provided by the *Drosophila* genome project.

Materials and methods

Strains and chromosomes

All fly strains were raised at 25°C unless otherwise stated. The two deficiency chromosomes used for the genetic analyses in this study, *Df(3L)Fpa1 th st sr cu* (Couderc et al. 2002) and *Df(3L)bab*^{PG} *e*^{s} *ry ca* (Godt et al. 1993), span the chromosomal regions 61D1–2 to 61F1–2 and 61D3-E1 to 61F5–8, respectively, and thus partially overlap. Both deficiencies uncover the *trio* locus. *Df(3L)Fpa2* (Couderc et al. 2002) and *Df(3L)Ar11* (H. M. Ellis, personal communication to FlyBase), spanning 61F1 to 61F4 and 61C3–4 to 61E, respectively, overlap *Df(3L)bab*^{PG}. *Df(3L)emc-E12*, which uncovers the region 61A to 61D3, is viable over *Df(3L)bab*^{PG}. *l(3)S036810* (Deak et al. 1997) is a P-element insertion allele of *trio* and 72% of the homozygotes develop to the adult stage. The P element is inserted in an intron that interrupts the coding sequence for amino acid 1756 in the *trio* ORF (Awasaki et al. 2000; Liebl et al. 2000). *Df(3L)Fpa1* also uncovers the *emc* locus at 61D1–2.

Cytology

Flies carrying deficiency chromosomes of the genotype *Df(3L)Ar11, red*^{1}*/TM6, Sb Tb*, *Df(3L)Fpa1/TM6B, Tb*, *Df(3L)bab*^{PG}*/TM6B, Tb* or *Df(3L)Fpa2/TM6B, Tb* were outcrossed to Canton S flies at 18°C, and the polytene chromosomes of third-instar larvae lacking the *Tb* marker present on the *TM6* balancer chromosomes were prepared for cytological analyses as described by Ashburner (1989). In situ hybridization to polytene chromosomes was carried out using digoxigenin-labeled *trio* cDNA as a probe.

Mutagenesis

w; e red males were treated with EMS as previously reported (Grigliatti 1986) and successively mated to *w; PrDr/TM6, Sb Tb* virgins. Single F1 males balanced with *TM6, Sb Tb* were crossed to *Df(3L)Fpa1/TM6B* virgins and lethality of the *Tb*$^{+}$ progenies was examined. From a total of 8890 mutagenized chromosomes 48 independent lethal mutations that failed to complement *Df(3L)Fpa1* were recovered. These mutations were mapped by crosses with *Df(3L)bab*^{PG} and a *trio* P-element insertion allele, *l(3)S036810* which allowed the identification of 22 mutations as *trio* alleles, and were further crossed to each other for assignment to distinct complementation groups.

To identify mutant embryos, larvae and adults in several experiments, the balancer chromosomes *TM6B, Abd-lacZ* and *TM6B, Ubi-GFP* were used to label non-mutant individuals by transgene expression, while *TM6, Sb Tb* animals were recognized on the basis of the dominant morphological markers.

Determination of lethal phases

The chromosomes carrying *Df(3L)Fpa1* or each EMS mutation were balanced over *TM6* harboring *Ubi-GFP*, so that the embryos bearing a mutant chromosome over *Df(3L)Fpa1* do not zygotically express GFP. However, the maternal contribution of GFP, due to the activity of the ubiquitin promoter during oogenesis, persisted even in late embryos, and therefore recognition of mutant animals was only possible at the late embryonic stage immediately prior to hatching, or during the first instar. The hatching rate was calculated as the number of hatched GFP-negative larvae relative to the sum of GFP-negative embryos and hatched larvae. The progeny were scored for up to 30 h or more after egg laying.

Western analysis

Western blot analyses were performed essentially as previously described (Awasaki et al. 2000). Whole adult bodies were homogenized in SDS sample buffer (3% SDS, 100 mM TRIS-HCl pH 8.0, 10% glycerol, 1 mM phenylmethylsulfonyl fluoride, 10 mM dithiothreitol, 1% Triton X-100, 10 mM $MgCl_2$, 100 mM NaCl, 50 μg/ml aprotinin). The samples were boiled for 5 min, centrifuged to remove cell debris, and electrophoresed on a 5–20% gradient SDS-polyacrylamide gel. The fractionated proteins were electroblotted onto a Hybond ECL membrane (Amersham Pharmacia). The membrane was blocked by incubation in PBTw (PBS + 0.1% Tween 20) containing 1.5% skim milk and 1.5% BSA for 1 h, and incubated with the antibody αTrioB6 raised against amino acids 1697–1925 of the Trio protein (1:1000; Awasaki et al. 2000). After three 15-min washes with PBTw, the membrane was incubated with horseradish peroxidase-conjugated anti-rabbit IgG antibody (Jackson Laboratories) for 1 h. After three washes, the signal was detected with the ECL system (Amersham Pharmacia).

Immunocytochemistry

Staining of wholemount embryos with monoclonal anti-Fasciclin II antibody (MAB1D4, Van Vactor et al. 1993) was performed as described by Awasaki et al. (2000).

Results

Isolation of new lethal EMS-induced mutations in the chromosomal region 61D1–2 to 61F1–2

In situ hybridization to polytene chromosomes revealed that *trio* maps at position 61E on the third chromosome. Several deficiencies are available that lack parts of this cytological region; *Df(3L)Ar11* extends from 61C3–4 to 61E, *Df(3L)Fpa1* from 61D1–2 to 61F1–2, *Df(3L)bab*^{PG} from 61D3-E1 to 61F5–8, and *Df(3L)Fpa2* from 61F1 to 61F4 (Godt et al. 1993). To determine which deficiencies uncover the *trio* locus, we performed in situ hybridization to polytene chromosomes of larvae that carried each deficiency over the wild-type chromosome. While the hybridization signals were detected all along the cytological band at 61E in the chromosomes of *Df(3L)Ar11*/ + and *Df(3L)Fpa2*/ + larvae (Fig. 1A and D), only a portion of the band was labeled in *Df(3L)Fpa1*/ + and *Df(3L)bab*^{PG}/ + individuals (Fig. 1B and C), demonstrating that *trio* is uncovered by the region of overlap between the latter two deficiencies. We therefore chose *Df(3L)Fpa1* for a systematic mutagenesis screen to recover lethal mutations, primarily with the intention of isolating *trio* alleles.

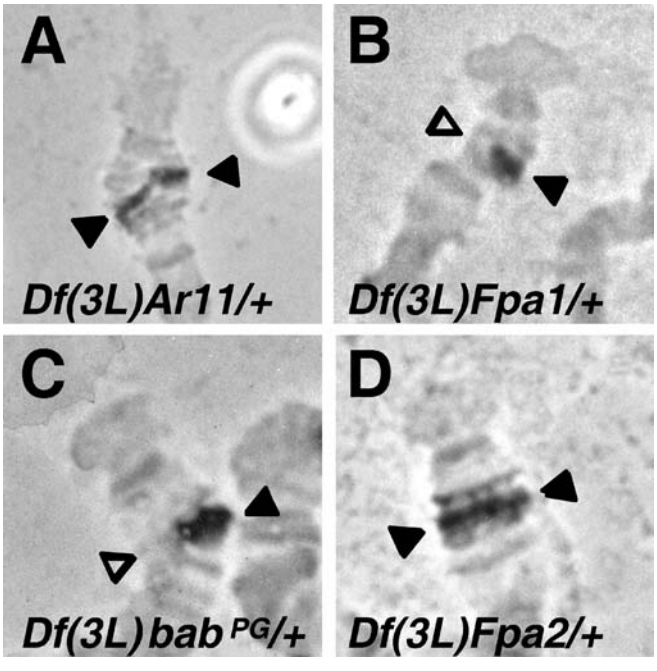

Fig. 1A–D Mapping of the *trio* locus on polytene chromosomes. The *filled* and *open arrows* indicate the presence and absence of the *trio* locus, respectively, as revealed by in situ hybridization. Note the absence of a hybridization signal on both the *Df(3L)Fpa1* (**B**) and *Df(3L)bab*^{PG} (**C**) chromosomes

A total of 8890 third chromosomes mutagenized with EMS were screened for lethality over *Df(3L)Fpa1*, resulting in the isolation of 48 new lethal mutations. The frequency of lethal mutations in this region was thus one per 185 chromosomes screened. All these mutations were crossed to the overlapping deficiency, *Df(3L)bab*^{PG}, and were further mapped to either the proximal or distal section of *Df(3L)Fpa1* by scoring lethality of the progenies. The mapped mutations were successively assigned to complementation groups by inter se crosses within each section. These procedures revealed that there are eight lethal genes in the interval 61D1–2 to 61F1–2. The results are summarized in Fig. 2 and Table 1.

Lethal mutations that mapped to the distal section of *Df(3L)Fpa1* defined six lethal genes. While the Berkeley *Drosophila* Genome Project has predicted more than ten genes in this region (Adams et al. 2000), complete assignment of the mutations to these putative genes has not been accomplished. However, we found by a genetic cross that *Df(3L)Fpa1* uncovers *emc*, raising the possibility that the locus may be one of the six lethal loci. Indeed, we found that the single allele of the complementation group *61Da* recovered, *G4.1*, failed to complement *emc*^{1} for embryonic lethality, demonstrating that *61Da* corresponds to *emc*. Moreover, a P-element insertion, *l(3)00835* (Spradling et al. 1995, 1999), which was lethal over *Df(3L)Fpa1*, failed to complement the *K1.2* allele of *61Db* and all three alleles (*B1.1*, *S2.1* and *2J1.1*) of *61Dc* to varying extents (Fig. 3). These genetic findings suggest that the two loci may be physically close to each other so that a single P-element insertion may impair the function of both genes. The BDGP has previously determined that the insertion is located about 300 bp upstream of the predicted gene *CG13900* and 1 kb upstream of the adjacent gene *CG13886* (Fig. 2). Therefore, the two loci are likely to correspond to *CG13900* and *CG13866*, although a one-to-one assignment could not be achieved. None of other P-element insertions previously reported to lie in this region showed lethality over the mutations isolated in the present study.

Lethal mutations that mapped to the proximal section of *Df(3L)Fpa1* defined two lethal genes, *61Ea* and *61Eb*. The mutations in *61Ea* were found to be lethal over *l(3)S007412* (Deak et al. 1997). Based on information in Flybase, we noticed that this P-element insertion lies within the intron of the *Glut1* gene (Escher and Rasmuson-Lestander 1999). Since no overlapping genes have been predicted in this region, *61Ea* and *l(3)S007412* are most likely to represent *Glut1*, which encodes a putative glucose transporter. An inversion mutation, *In(3LR)208*, with breakpoints at 61E2–3 and 86C1–2 (Craymer 1984; Coyne et al. 1993), failed to complement *l(3)S007412* for lethality, indicating that one of the break points disrupts *Glut1* (Fig. 2).

For the last complementation group, *61Eb*, 22 mutations were isolated, suggesting that the gene extends over a large region. We previously found that a P-element insertion, *l(3)S036810* (Deak et al. 1997), maps in an intron of the *trio* gene (Awasaki et al. 2000; Liebl

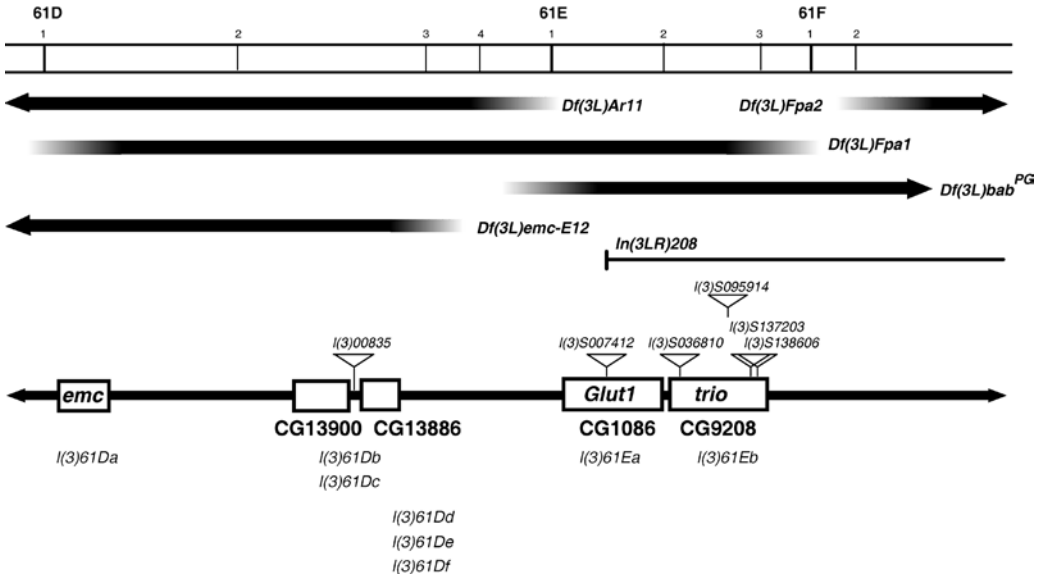

Fig. 2 Cytological map showing the extent of the aberrations used and the distribution of recessive lethals in the region 61D1–2 to 61F1–2. The six complementation groups located in the distal region (61D) of *Df(3L)Fpa1* complement *Df(3L)bab*^{PG}, but not *Df(3L)Ar11*, while the two groups in the proximal region (61E), *l(3)61Ea* and *l(3)61Eb*, complement *Df(3L)Ar11*, but not *Df(3L)bab*^{PG}. Although more than twenty transcripts are predicted by Genome Sequencing Project (Adams et al. 2000) in this region, only the four genes shown with CG numbers are associated with P-element insertions. The *l(3)00835* insertion is located close to both *CG13900* and *CG13886*, which presumably correspond to *l(3)61Db* and *l(3)61Dc*, because the single insertion impairs both loci (see Fig. 4). However, these loci have not been ordered with respect to each other. Note that one of the breakpoints of *In(3LR)208* disrupts *Glut1*. Attempts to assign *l(3)61Dd*, *l(3)61De* and *l(3)61Df* to other predicted genes have so far been unsuccessful

et al. 2000). Individuals carrying this allele over *Df(3L)Fpa1* showed reduced viability, and this phenotype could be rescued by expressing the *trio* cDNA under the control of a heat shock promoter (Awasaki et al. 2000). All 22 mutations isolated in the present study failed to complement *l(3)S036810*, indicating that *61Eb* corresponds to the *trio* gene. In addition, it has been reported that *l(3)S095914*, *l(3)S137203* and *l(3)S138606* (Deak et al. 1997) are other alleles of this gene (Bateman et al. 2000; Newsome et al. 2000).

Characterization of the *trio* mutations

We have examined the morphological phenotypes conferred by each of the 22 *trio* mutations. The mutant animals [*trio*/*Df(3L)Fpa1*] appeared normal in overall structure during embryonic stages, but most died during the larval stages. We expected that *trio* mutant embryos might have defects in the nervous system, because *Df(3L)Fpa1*/*Df(3L)bab*^{PG} embryos show severely disrupted patterns of axon wiring (Fig. 4B), as revealed by staining with the anti-Fasciclin II monoclonal antibody,

Table 1 Summary of complementation groups

Locus (synonym)	Phenotypic class[a]	Lethal phase[b]	Known genetic lesions	Newly isolated alleles
l(3)61Da (*emc*)	Lethal	E	See FlyBase[c]	*G4.1*
l(3)61Db	Lethal	PA	*l(3)00835*	*K1.2*
l(3)61Dc	Lethal	EL	*l(3)00835*	*B1.1*, *S2.1*, *2J1.1*
l(3)61Dd	Lethal	EL		*2F1.1*, *2G1.1*, *2K2.1*
l(3)61De	Lethal	LP		*2P3.1*, *2P3.2*, *2V3.1*, *K3.1*
l(3)61Df	Semilethal/lethal[d]	PA		*A3.2*, *A4.1*, *G1.1*, *K1.1*, *M1.1*, *N3.1*[d], *Q2.1*, *T1.1*, *2G4.1*, *2J3.2*, *2R2.1*
l(3)61Ea (*Glut1*)	Lethal	PA	*l(3)S007412*, *In(3LR)208*	*2M1.1*, *2Q2.1*, *2π1.1*
l(3)61Eb (*trio*)	Lethal	L	*l(3)S036810*, *l(3)S095914*, *l(3)S137203*, *l(3)S138606*	*BD1.1*, *E4.1*, *L4.1*, *M2.2*, *M4.1*, *O3.1*, *S2.2*, *U1.1*, *V2.1*, *2D2.1*, *2E2.1*, *2H3.1*, *2J3.1*, *2M3.1*, *2S4.2*, *2T2.1*, *2T4.1*, *2T4.2*, *2U4.1*, *2Y1.1*, *2Z4.1*, *2p2.1*

[a]Each allele was examined for lethality when placed in *trans* to *Df(3L)Fpa1*. Lethal, viability < 5%; semilethal, viability < 50%
[b]E, embryonic; L, larval; P, pupal; A, adult
[c]Available at http://flybase.bio.indiana.edu/
[d]The viability of N3.1 was 0%, but animals with other alleles developed to adulthood. The survival rate varied from 5.7% (*A4.1*) to 53.8% (*T1.1*)

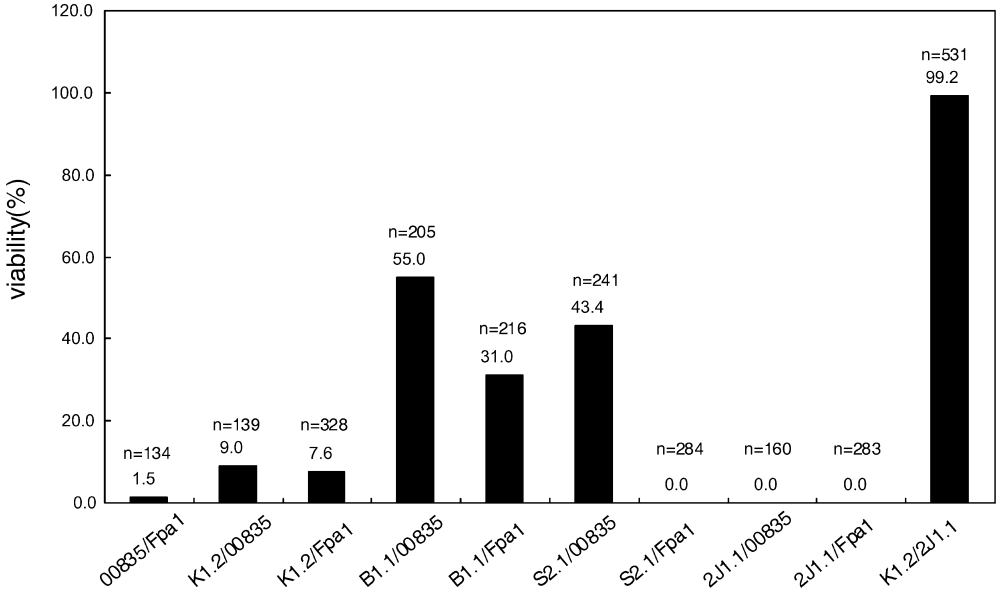

Fig. 3 Effects of the mutation *l(3)00835* on the loci *61Db* and *61Dc*. The P-element insertion *l(3)00835* failed to complement both *61Db* (*K1.2*) and *61Dc* (*B1.1*, *S2.1* and *2J1.1*) to varying extents. Note that *K1.2* fully complements *2J1.1*, which indicates that these alleles belong to different complementation groups. "00835" and "Fpa1" represent *l(3)00835* and *Df(3L)Fpa1*, respectively. The number (n) of flies scored is shown *above* each *bar*

MAB1D4 (Van Vactor et al. 1993). This antibody stains three longitudinal fascicles on each side of the ventral nervous system of wild-type embryos at stage 16/17 (Fig. 4A). In contrast, all the *trio* mutant embryos analyzed in this study showed abnormal patterning of the longitudinal fascicles, as previously observed for $trio^{E4.1}$ (Awasaki et al. 2000); the outermost fascicles were discontinuous and fused to the adjacent inner fascicles (Fig. 4C). Since $trio^{E4.1}/trio^{E4.1}$ and $trio^{E4.1}/Df(3L)Fpa1$ embryos exhibited similar degrees of aberration, the phenotype possibly represents the consequence of complete or almost complete loss of *trio* activity. It should be noted, however, that the phenotype of *trio* homozygotes is much milder than that observed in $Df(3L)Fpa1/Df(3L)bab^{PG}$ embryos, suggesting the lack of additional functions within the region of overlap is responsible for the severe axonal patterning phenotype of the deficiency embryos.

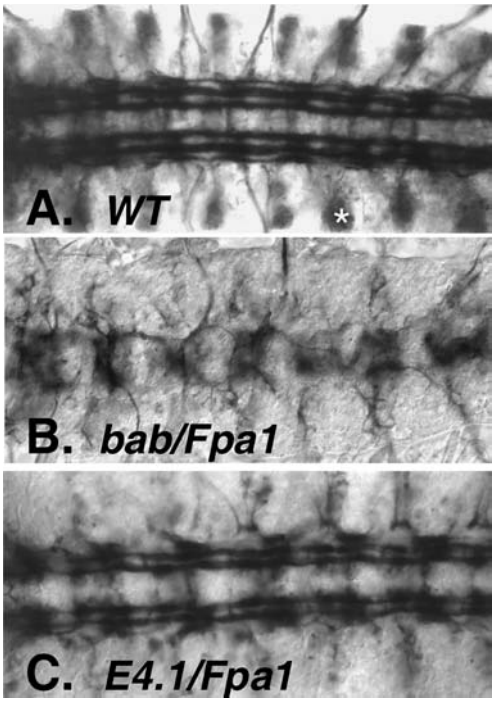

Fig. 4A–C Axon wiring patterns in the CNS of stage 17 embryos stained with anti-Fasciclin II antibody. **A** Wild-type embryo. Three longitudinal connectives are arranged on each side of the ventral midline. The *asterisk* indicates *lacZ* staining. **B** $Df(3L)bab^{PG}/Df(3L)Fpa1$ embryo. No longitudinal fascicles are visible. **C** $trio^{E4.1}/Df(3L)Fpa1$ embryos. The outermost fascicles are disrupted, but inner fascicles have formed. Anterior is to the *left*

To further characterize the *trio* alleles, we examined the expression of Trio protein in the mutants by Western analysis (Fig. 5). An anti-Trio antibody, αTrioB6, labeled multiple bands, but three major bands (one at >200 kDa and a doublet at 130 kDa) could be identified as Trio proteins, because they were not detectable in the *l(3)S036810* homozygotes. Then we examined flies carrying each of the *trio* mutations over *l(3)S036810*. In 13 of 17 mutations examined, the >200-kDa band was absent, with the smaller major bands remaining apparently unchanged. In agreement with this, one of these mutations, $trio^{E4.1}$, is a 1-bp substitution that generates a stop codon at amino acid 261, as revealed by our previous sequence analyses (Awasaki et al. 2000), truncating the >200-kDa protein to a small product that was not detectable in our Western analyses (Fig. 5). These data suggested that the >200-kDa product is essential for correct axonal patterning in the ventral nervous system of embryos, as well as for viability during the larval stages. In contrast, four other mutations still exhibited the >200-kDa product at varying intensities. For instance, the product was detected at the normal level for $trio^{L4.1}$ and $trio^{2E2.1}$, but faintly for $trio^{M2.2}$ and $trio^{M4.1}$. It is likely that $trio^{L4.1}$ and $trio^{2E2.1}$ are missense mutations in the frame encoding the >200-kDa protein, and that $trio^{M2.2}$ and $trio^{M4.1}$ may be altered in regula-

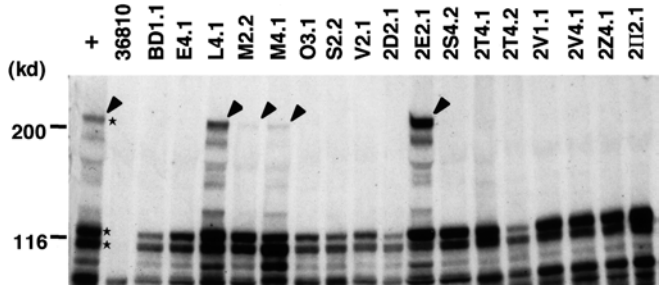

Fig. 5 Western analysis of *trio* mutants. Extracts were prepared from wild type (+), *l(3)S036810/l(3)S036810*, and individuals bearing each *trio* allele over *l(3)S036810*. Molecular weights are indicated on the *left*. The *asterisks* mark the major bands labeled with anti-Trio antibody (αTrioB6). Note that these major and minor bands disappear in *l(3)S036810/l(3)S036810* animals. The largest band, marked by the *filled arrowheads*, is undetectable in many mutants, and is greatly decreased in amount in $trio^{M2.2}$/*l(3)S036810* and $trio^{M4.1}$/*l(3)S036810*, but remains apparently intact in $trio^{L4.1}$/*l(3)S036810* and $trio^{2E2.1}$/*l(3)S036810*. No significant changes in the smaller major bands were detected for any mutant alleles except for *l(3)S036810*

tory sequences important for either transcription or translation.

While the >200-kDa protein was affected in size and amount in many of the mutants isolated in our screen, no apparent alteration was found in the small major proteins in any of the mutants. This observation suggests that the small products are not involved in mutant lethality and may indeed be dispensable for viability.

Phenotypic characterization of the lethal complementation groups

When crossed with flies carrying *Df(3L)Fpa1*, all the mutants isolated in this study, except for the *emc* allele, *G4.1*, produced eggs that developed through all embryonic stages, but the hatched larvae died at various later stages (Table 1). None of the hatching mutant embryos exhibited gross morphological alterations. We stained embryos with MAB1D4 to examine the motor nerve pathways and subsets of longitudinal axon tracts in the central nervous system, and found that the nervous system in the mutants was apparently normal, although minor defects could not be ruled out. MAB1D4 staining was also performed on central nervous systems dissected from the mutant first-instar larvae, and revealed again that the longitudinal axon tracts were arranged in an essentially correct pattern (data not shown). Thus, the genes targeted by these mutations are not involved in basic morphogenesis or in nervous system development during embryonic and early larval stages.

Among these complementation groups, two loci, *l(3)61Db* and *l(3)61Df*, were represented by semilethal alleles. Some 7% of mutant animals bearing the *K1.2* allele of *l(3)61Db* over *Df(3L)Fpa1* survived to adulthood, and the escaper flies exhibited uncoordinated movements. For the *l(3)61Df* locus, eleven mutant alleles were isolated, which show survival rates that varied from 0% (*N3.1*) to about 50%. Some 5.3% of flies carrying a strong allele, *A3.2*, over *Df(3L)Fpa1* developed to the adult stage, and these also exhibited uncoordinated locomotion.

While these mutations did not produce any gross morphological aberrations in embryos, an *emc* allele, *G4.1*, caused the mutant animals to die during embryonic stages with clear developmental defects (Fig. 6). *G4.1/Df(3L)Fpa1* embryos looked normal at early embryonic stages. However, it became clear at stage 17 that the shapes of the head and midgut were abnormal. In wild-type embryos, the pharyngeal muscle evident at stage 15 is gradually covered by the dorsal fold and internalized as development proceeds (Fig. 6A). The midgut undergoes constriction to form three compartments by the end of stage 16. In contrast, we found that, in the mutant, head development was retarded around stage 15; the dorsal fold did not migrate anteriorly, so that the pharyngeal region remained exposed as an anterior protrusion on the dorsal side of the head even after denticle belts had formed (Fig. 6B). The midgut also failed to develop and, in typical cases, appeared as a thick smooth tube without constrictions (Fig. 6B). Moreover, dorsal closure did not proceed normally, so that the dorsal midline was inappropriately shaped, pinched or puckered (Fig. 6D). In the central nervous system (CNS) of the mutant embryos, FasII-positive longitudinal tracts appeared normal, although the whole structure of the ventral ganglion failed to condense fully (data not shown). *G4.1/G4.1* embryos exhibited phenotypes similar to those of *G4.1/Df(3L)Fpa1* embryos (data not shown), suggesting that *G4.1* is a null allele of the *emc* locus.

Discussion

We have screened for lethal genes in the chromosomal region 61D1–2 to 61F1–2, primarily with the aim of isolating new *trio* alleles, using the deficiency *Df(3L)Fpa1*, which uncovers the *trio* locus. Our complementation analyses indicated that this region, with nine cytological bands, contains eight essential genes including *trio*, *Glut1* and *emc*. We isolated 22 alleles for the *trio* locus, single alleles for *emc* and *61Db*, and several alleles each for the other complementation groups. These numbers are compatible with the fact that *trio* is a large locus, and also suggest that the mutations identified in this study represent most, if not all, genes in the chromosomal interval of interest.

However, during the analyses of the mutant phenotypes, it emerged that at least one lethal gene may remain to be identified in the interval of interest. In order to map the *trio* locus more precisely, we employed $Df(3L)bab^{PG}$ for genetic crosses, which overlaps with the proximal part of *Df(3L)Fpa1*. The $Df(3L)bab^{PG}$/*Df(3L)Fpa1* embryos exhibited severe wiring defects in the embryonic CNS, as revealed by FasII staining.

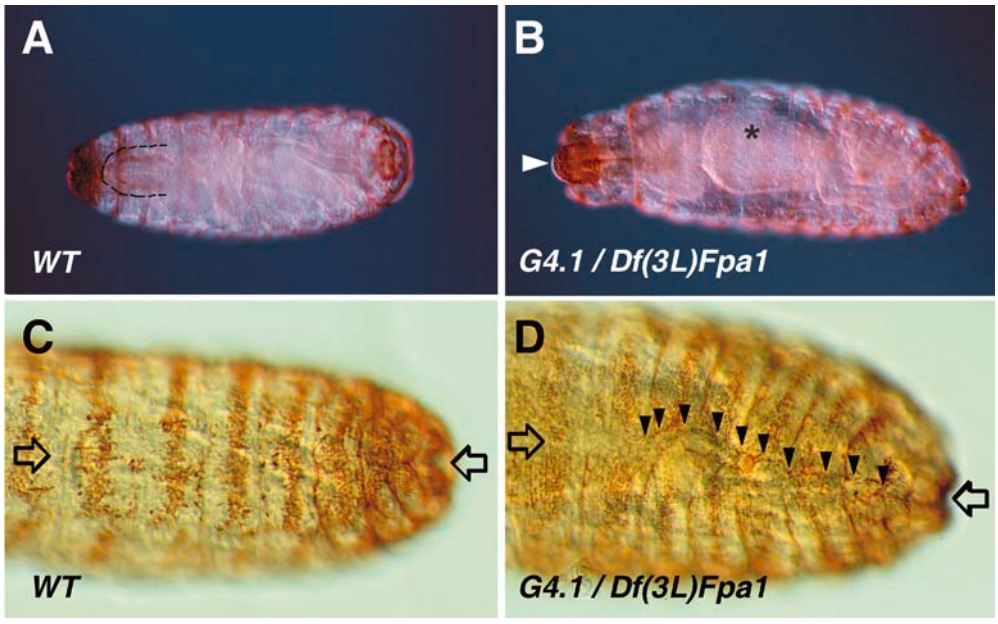

Fig. 6A–D Morphological aberrations in *G4.1* embryos. Wild-type (**A** and **C**) and *G4.1* (**B** and **D**) embryos were stained with MAB1D4 to visualize several tissues. Anterior is to the *left* and dorsal is *up*. **A** In a stage 17 wild-type embryo, the pharyngeal region (*broken line*) is fully internalized. The internal organs are densely packed. **B** In a *G4.1* embryo, the pharyngeal region (*white arrowhead*) is improperly positioned, remaining exposed as an anterior protrusion. The midgut (*asterisk*) has no constrictions. The presence of secreted cuticle indicates that this embryo has reached the final stage of embryogenesis. **C** A stage 17 wild-type embryo. The *open arrows* indicate the dorsal midline. Note that the cuticle is seamless. **D** A *G4.1* embryo. The dorsal midline is marked with *black arrowheads*. The line is pinched or curved, and the dorsal surface is puckered

However, we did not find this phenotype in any embryos of the mutant strains isolated in this study. The most similar phenotype was observed in the *trio* embryos, in which the three longitudinal connectives stained by FasII were fused to each other, but this aberration was much milder than that of $Df(3L)bab^{PG}/Df(3L)Fpa1$ embryos. There are two possible explanations for this inconsistency. First, the simultaneous loss of function of the few genes localized in the region of overlap between the two deficiencies may produce severe morphological defects in the CNS. In this case, given that *trio* is involved in the phenotype, we should be able to rescue or ameliorate it by expressing *trio* cDNA under the control of an appropriate promoter. We introduced *UAS-trio* driven by *elav-Gal4* into $Df(3L)bab^{PG}/Df(3L)Fpa1$ embryos and found that the mutant phenotype in the CNS was not rescued (our unpublished data). This observation suggested that *trio* does not contribute very much to the observed structural abnormality. Nevertheless, it is still possible that *Glut1* and/or other unidentified non-lethal genes in the overlap between the two deficiencies synergistically interact with each other to produce the severe phenotype. Alternatively, the *Df(3L)Fpa1* chromosomal region may not have been saturated with lethal mutations in our mutagenesis experiment. Therefore, one or more essential genes whose loss greatly disrupts the axonal wiring pattern may not have been identified. It remains to be determined which of these possibilities accounts for the mutant phenotype observed in $Df(3L)bab^{PG}/Df(3L)Fpa1$ embryos.

Of the 48 alleles in eight complementation groups identified in this study, only the alleles in two complementation groups, *trio* and *emc*, caused morphological defects in the embryos. For *trio*, 22 alleles were identified by complementation tests that were performed successively with *Df(3L)Fpa1*, $Df(3L)bab^{PG}$ and *l(3)S036810*. All of the alleles examined exhibited essentially the same phenotype in the wiring pattern of the embryonic CNS, and the same defect was observed in both homozygous mutant embryos and in *trans* to *Df(3L)Fpa1* for many alleles, suggesting that these mutations represent strong or null alleles. These genetic data, together with our Western analyses, demonstrate that *trio* plays a pivotal role in the regulation of axon extension or guidance.

G4.1 was isolated as a new *emc* allele that caused severe morphological aberrations in embryos. *emc* encodes an HLH protein that regulates sensory organ precursor formation by its ability to form inactive heterodimers with the bHLH products of the *achaete-scute* complex and/or *daughterless* (Botas et al. 1982; Garcia-Alonso and Garcia-Bellido 1988; Van Doren et al. 1992). In addition to its role in the formation of sensory organ precursors, the *emc* function is required for normal development of the midgut, Malpighian tubules and head, suggesting that negative regulation by Emc may be a common feature of many developmental processes (Cubas et al. 1994; Ellis 1994). Our finding that *G4.1* embryos had defects in head involution and midgut formation, and newly discovered lesions in ventral ganglion condensation and dorsal closure, is compatible with this notion.

It was previously shown that the cuticle structure of *emc* mutant embryos displays alterations in the head region (Cubas et al. 1994). The larval head is formed by the internalization of the anterior head region of developing embryos, and this involves a complex and highly ordered set of cell rearrangements. In the *G4.1* embryos, we found that the dorsal fold stopped migrating anteriorly, and the pharyngeal tissues remained externally exposed as a frontal protrusion. The head structure in the older mutant embryos resembled that of stage 15 wild-type embryos, suggesting that head involution ceased around this stage. Thus, *emc* has a critical function in regulating the dynamic processes of head involution.

By the end of stage 15, wild-type embryos complete dorsal closure, making the dorsal midline straight and eventually seamless. In *G4.1* embryos, however, while dorsal closure is largely completed, the epithelial sheets failed to fuse smoothly at the dorsal midline and became puckered. It has been shown that dorsal closure is regulated by DJNK, Dpp and Rho1 signaling pathways. For example, in the DJNK cascade, several factors, including protein kinases, a phosphatase and transcription factors, are known to control continuous cell movement by regulating the proper organization of actin, myosin and phosphotyrosine-containing proteins in the cells at the leading edge (see, for example, Martin-Blanco et al. 1998). Moreover, components of the Dpp-mediated signal transduction pathway that include the receptor protein kinases and transcription factors are also involved in the event (see Simin et al. 1998). Finally, the Rho1 pathway that includes Pkn controls dorsal closure, possibly in a manner independent of the JNK and Dpp pathways (Lu and Settleman 1999). Thus, one or more of these signal transduction pathways may regulate the expression or activity of *emc*, or conversely *emc* may act upstream of these pathways. It may be noteworthy that *Rho1* embryos exhibit head involution defects, as well as a puckered dorsal surface due to improper dorsal closure (Magie et al. 1999); both of these features are also found in *G4.1* mutant embryos. Therefore, a link between the Rho1 pathway and *emc* may be a more plausible possibility. Further genetic and biochemical experiments will be required, however, to determine which pathway relays a signal to or from *emc* during the process of dorsal closure.

In this study, we performed a systematic lethal screen of the genomic region 61D1–2 to 61F1–2, and identified eight loci including *trio*, *Glut1* and *emc*. Future detailed analysis of the mutant phenotypes will disclose the functions of these genes, and thereby contribute to understanding the functions of all essential genes and, ultimately, the whole genetic system of *Drosophila*.

Acknowledgements We greatly thank Frank Laski for fly stocks and sharing results prior to publication, the Bloomington and Szeged Stock Centers for fly stocks, and the Berkeley *Drosophila* Genome Project for genomic information. This study was supported by Core Research for Evolutional Science and Technology (Japan Science and Technology Corporation) and by Grants-in-Aid for Scientific Research on Priority Areas (A) and (C) (“Genome Science” and “Advanced Brain Science Project”) from the Ministry of Education, Culture, Sports, Science and Technology of Japan.

References

Adams MD, et al (2000) The genome sequence of *Drosophila* melanogaster. Science 287:2185–2195

Ashburner MC (1989) Drosophila: a laboratory handbook. Cold Spring Harbor Laboratory Press, Cold Spring Harbor, N.Y.

Awasaki T, Saito M, Sone M, Suzuki E, Sakai R, Ito K, Hama C (2000) The Drosophila Trio lays an essential role in patterning of axons by regulating their directional extension. Neuron 26:119–131

Bateman J, Shu H, Van Vactor D (2000) The guanine nucleotide exchange factor Trio mediates axonal development in the Drosophila embryo. Neuron 26:93–106

Botas J, del Prado JM, Garcia-Bellido A (1982) Gene-dose titration analysis in the search of *trans*-regulatory genes in Drosophila. EMBO J 1:307–310

Couderc J-L, Godt D, Zollman S, Chen J, Li M, Cramton SE, Sahut-Barnola I, Laski FA (2002) The *bric à brac* locus consists of two paralogous genes encoding BTB/POZ domain proteins, and acts as a homeotic and morphogenetic regulator of imaginal development in *Drosophila*. Development 129:2419–2433

Coyne JA, Meyers W, Crittenden AP, Sniegowski PD (1993) The fertility effects of pericentric inversions in *Drosophila melanogaster*. Genetics 134:487–496

Craymer L (1984) Techniques for manipulating chromosomal rearrangements and their application to *Drosophila melanogaster*. Genetics 108:573–587

Cubas P, Modolell J, Ruiz-Gomez M (1994) The helix-loop-helix extramacrochaetae protein is required for proper specification of many cell types in the Drosophila embryo. Development 120:2555–2565

Deak P, et al (1997) P-element insertion alleles of essential genes on the third chromosome of *Drosophila melanogaster*: correlation of physical and cytogenetic maps in chromosomal region 86E–87F. Genetics 147:1697–1722

Dickson BJ (2001) Rho GTPases in growth cone guidance. Curr Opin Neurobiol 11:103–110

Ellis HM (1994) Embryonic expression and function of the Drosophila helix-loop-helix gene, *extramacrochaetae*. Mech Dev 47:65–72

Engels WR (1996) P elements in *Drosophila*. In: Saedler H, Gierl A (eds) Transposable elements. Springer-Verlag, Berlin, pp 103–123

Escher SA, Rasmuson-Lestander A (1999) The Drosophila glucose transporter gene: cDNA sequence, phylogenetic comparisons, analysis of functional sites and secondary structures. Hereditas 130:95–103

Garcia-Alonso LA, Garcia-Bellido A (1988) Extramacrochaetae, a *trans*-acting gene of the *achaete-scute* complex of Drosophila involved in cell communication. Roux Arch Dev Biol 197:328–338

Godt D, Couderc JL, Cramton SE, Laski FA (1993) Pattern formation in the limbs of *Drosophila*: *bric a brac* is expressed in both a gradient and a wave-like pattern and is required for specification and proper segmentation of the tarsus. Development 119:799–812

Grigliatti T (1986) Mutagenesis. In: Roberts DB (ed) *Drosophila*: a practical approach. IRL Press, Oxford, pp 39–58

Liebl EC., Forsthoefel DJ, Franco LS, Sample SH, Hess JE, Cowger JA, Chandler MP, Shupert AM, Seeger MA (2000) Dosage-sensitive, reciprocal genetic interactions between the Abl tyrosine kinase and the putative GEF trio reveal Trio’s role in axon pathfinding. Neuron 26:107–118

Lu Y, Settleman J (1999) The Drosophila Pkn protein kinase is a Rho/Rac effector target required for dorsal closure during embryogenesis. Genes Dev 13:1168–1180

Luo L (2000) Rho GTPases in neuronal morphogenesis. Nat Rev Neurosci 1:173–180

Magie CR, Meyer MR, Gorsuch MS, Parkhurst SM (1999) Mutations in the Rho1 small GTPase disrupt morphogenesis and segmentation during early *Drosophila* development. Development 126:5353–5364

Martin-Blanco E, Gampel A, Ring J, Virdee K, Kirov N, Tolkovsky AM, Martinez-Arias A (1998) *puckered* encodes a phosphatase that mediates a feedback loop regulating JNK activity during dorsal closure in *Drosophila*. Genes Dev 12:557–570

Newsome TP, Schmidt S, Dietzl G, Keleman K, Asling B, Debant A, Dickson BJ (2000) Trio combines with Dock to regulate Pak activity during photoreceptor axon pathfinding in Drosophila. Cell 101:283–294

Simin K, Bates EA, Horner MA, Letsou A (1998) Genetic analysis of Punt, a type II Dpp receptor that functions throughout the *Drosophila melanogaster* life cycle. Genetics 148:801–813

Spradling AC, Stern DM, Kiss I, Roote J, Laverty T, Rubin GM (1995) Gene disruptions using P transposable elements: an integral component of the *Drosophila* genome project. Proc Natl Acad Sci USA 92:10824–10830

Spradling AC, Stern D, Beaton A, Rhem EJ, Laverty T, Mozden N, Misra S, Rubin GM (1999) The Berkeley *Drosophila* Genome Project gene disruption project: single P-element insertions mutating 25% of vital *Drosophila* genes. Genetics 153:135–177

Van Doren M, Powell PA, Pasternak D, Singson A, Posakony JW (1992) Spatial regulation of proneural gene activity: auto- and cross-activation of *achaete* is antagonized by *extramacrochaetae*. Genes Dev 6:2592–2605

Van Vactor D, Sink H, Fambrough DM, Tsoo R, Goodman CS (1993) Genes that control neuromuscular specificity in Drosophila. Cell 73:1137–1153